Hybrid Strategies for Adjoint Methods in the Context of Shape Optimization

Seminararbeit von

Fabian Key
(303550)

Juli 2014

Betreuer: Dipl.-Ing. M. Towara (STCE)

STCE
RWTH Aachen University
Germany

Contents

1 Introduction **2**
1.1 Task Description 2
1.2 Shape Optimization 2

2 Adjoint Methods **4**
2.1 The Discrete Approach 5
2.2 The Continuous Approach 6
2.3 The Hybrid Approach 7

3 Application to Turbulent Flow Simulations **9**
3.1 Problem Description 9
3.2 Results 12

4 Conclusion **15**

List of Figures

1.1 Hicks-Henne bump functions $h(x) = \left(\sin(\pi x^{\frac{\log 0.5}{\log a}})\right)^3$ for $a = 0.25, 0.5, 0.75$. 3
1.2 Optimization loop using an adjoint method 3

2.1 Discretization and linearization compared for the discrete and continuous adjoint approach [6] 4
2.2 Simple comparison of the different approaches [6] 7
2.3 Schematic sketch of the hybrid adjoint approach [6] 7

3.1 Computational mesh around the airfoil [6] 9
3.2 Surface sensitivity of drag coefficient [6] 12
3.3 Shape sensitivity of drag coefficient [6] 13
3.4 Drag and lift coefficient during the shape optimization process [6] 14
3.5 Comparison of original and optimized shapes after 10 design steps [6] 14

List of Symbols

a	Parameter of Hicks-Henne bump function.
$\mathcal{C}$	Subscript for continuous approach.
C_p	Specific heat capacity for constant pressure.
D	Subscript for discrete approach.
E	Internal energy.
F	Flux term.
f	Function for eddy viscosity.
F^{v1}	First viscous flux term.
F^{v2}	Second viscous flux term.
$\mathcal{G}$	Constraints.
H	Stagnation enthalpy.
$h(x)$	Hicks-Henne bump function.
$\mathcal{J}$	Cost functional.
$\mathcal{L}$	Lagrangian function.
L	Lagrangian function.
M_∞	Dimensionless freestream Mach number.
n	normal vector.
p	Static pressure.
Pr	Dimensionless Prandtl number.
Pr_T	Dimensionless turbulent Prandtl number.
$\mathcal{R}$	Gas constant.
$\mathcal{N}$	Continuous constraints or PDEs.
$\mathcal{R}$	Discrete constraints or residuals.
Re	Dimensionless Reynolds number.
T	Static temperature.
U	State variables.
u	Velocity.
$\mathcal{V}$	Lagrange multipliers or adjoint variables.
α	Design variables.
$\hat{\alpha}$	Angle of attack.
β	Switch for hybrid cost functional.
Γ	Boundary of domain.
δ_{ij}	Kronecker delta function.
$\delta()$	Continuous perturbation.
$\Delta()$	Discrete perturbation.
$\{\delta,\Delta\}\,()$	Hybrid perturbation.
μ	Laminar viscosity.
μ_t	Turbulent viscosity.
μ^{v1}	First viscosity combination.
μ^{v2}	Second viscosity combination.
ρ	Density.
τ	Stress tensor.
ϕ	Discrete adjoint variables.
φ	Hybrid adjoint variables.
Ψ	Discrete adjoint variables.
Ω	Computational domain.

1 Introduction

1.1 Task Description

This paper was produced during the summer term 2014 in the context of the *CES Master Seminar*. The task was to deal with a topic of current research based on scientific papers. Emphasis should be put on a didactic and comprehensible description of the selected issue.

In this paper, the principles of adjoint based shape optimization are considered. Particularly, the utilization of a hybrid adjoint approach is motivated and discussed. This work mainly presents the findings published by Taylor et al. [5],[6].

1.2 Shape Optimization

Shape optimization is the task to find a shape of a geometry that is *optimal* regarding a specific cost functional $\mathcal{J}$. Typically, the shape has to satisfy a set of given constraints $\mathcal{G} = 0$ at the same time. Often, these constraints are defined by partial differential equations (PDEs) $\mathcal{N} = 0$, which have to be fulfilled on the computational domain Ω. The optimization problem is discretized by introducing a parametrization of the shape which is defined by a set of design variables α. Depending on the choice of parametrization, the design variables could be e.g. the parameters of Hicks-Henne sine bump functions [2] (see Figure 1.1) or the normal displacement of surface mesh elements.
The cost functional is typically defined over the domain Ω or the boundary Γ depending both on the state variables U and the design variables α:

$$\mathcal{J}(U, \alpha) \text{ on } \Omega \text{ or } \Gamma \tag{1.1}$$

The constraints can be combined as

$$\mathcal{G}(U, \alpha) = (\mathcal{N}) = 0 \text{ on } \Omega. \tag{1.2}$$

The constrained problem

$$\min_{\alpha} \mathcal{J}(U, \alpha) \text{ subject to } \mathcal{G}(U, \alpha) = 0 \text{ on } \Omega \tag{1.3}$$

can be transformed into an unconstrained optimization problem by the so called method of Lagrange multipliers. The Lagrangian function is defined as

$$\mathcal{L} = \mathcal{J} + \mathcal{V}^T \mathcal{G}, \tag{1.4}$$

where $\mathcal{V}$ denotes the Lagrange multipliers which will be referred to as adjoint variables in the following. For the solution of this problem, one can select an appropriate optimization method. Here, we want to refer to gradient based optimization methods like the steepest descent method. For these methods, the gradient of the Lagrangian function $\mathcal{L}$ with respect to design variables α is needed. It has as many entries as the number of design variables. The individual components are also called sensitivities, because they describe the change of the cost functional due to small changes in the corresponding design variable. One notes that the Lagrangian function consists of both the cost functional and the constraints defined by PDEs and, in general, depends on the design variables α as well as on the state variables U.

One way to calculate the sensitivities would be the finite differences approach. However, the computation of each component of the gradient would require the value of $\mathcal{L}$ and, thus, the solution of a PDE system for a perturbation in one specific design variable. Therefore, the overall effort for the gradient computation is proportional to the number of design variables.

Adjoint methods overcome this drawback and can provide sensitivity information at the

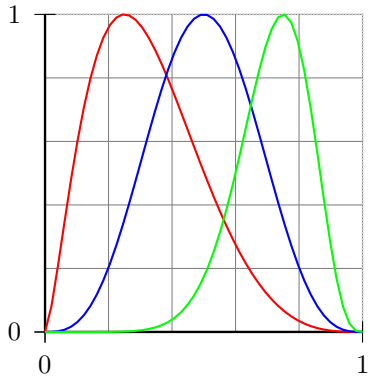

Figure 1.1: Hicks-Henne bump functions $h(x) = \left(\sin(\pi x^{\frac{\log 0.5}{\log a}})\right)^3$ for $a = 0.25, 0.5, 0.75$

costs of approximately one additional evaluation of $\mathcal{L}$ or solution of the PDEs defining the constraints.

According to the obtained sensitivities, the design parameters and, thus, the shape are adapted. Typically, also the corresponding computational mesh has to be updated to fit the new shape, but this topic is not considered here. For the updated shape, the equations which define the constraints (primal equations) have to be solved once more. Further, the adjoint solution is calculated and, again, sensitivities are computed and so forth. Finally, the optimization is an iterative process and it is illustrated in Figure 1.2

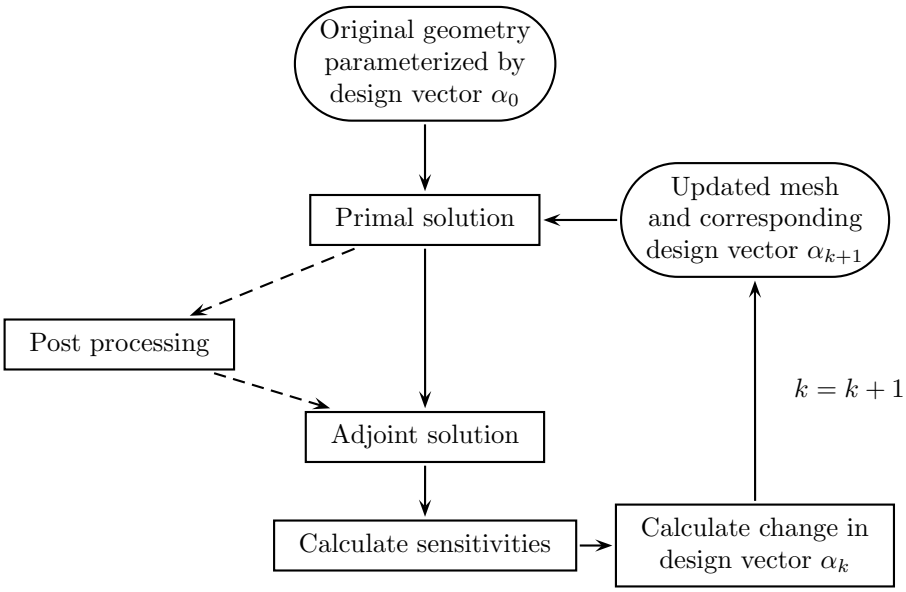

Figure 1.2: Optimization loop using an adjoint method

2 Adjoint Methods

Adjoint methods can be used to obtain sensitivity information used in gradient based optimization methods. One main advantage of these methods is that this information can be obtained at costs of one additional evaluation of $\mathcal{L}$ independent of the number of design variables.

The underlying derivation is outlined in the following. The perturbation of the Lagrangian $\delta\mathcal{L}$ arising from changes in the design α, which cause variations in the shape and, therefore, also in the state variables, is given as

$$\delta\mathcal{L} = \delta\mathcal{J} + \mathcal{V}^T \delta\mathcal{G}. \tag{2.1}$$

We can expand the terms of equation (2.1) introducing the perturbations of the state variables δU and those of the design variables $\delta\alpha$. Factorizing yields:

$$\delta\mathcal{L} = \left(\frac{\partial\mathcal{J}}{\partial\alpha} + \mathcal{V}^T\frac{\partial\mathcal{G}}{\partial\alpha}\right)\delta\alpha + \left(\frac{\partial\mathcal{J}}{\partial U} + \mathcal{V}^T\frac{\partial\mathcal{G}}{\partial U}\right)\delta U \tag{2.2}$$

Since we are still free in the choice of the adjoint variables $\mathcal{V}$, we can make a demand on these variables such that the explicit dependence of $\delta\mathcal{L}$ on perturbations in the state variables δU vanishes. Otherwise, these dependencies would oblige us to recompute the solution for the state variables for each perturbation in any design variable. These demands then result in the adjoint equation

$$\frac{\partial\mathcal{J}}{\partial U} + \mathcal{V}^T\frac{\partial\mathcal{G}}{\partial U} = 0. \tag{2.3}$$

If this equation and the constraints are fulfilled ($\mathcal{G} = 0 \Rightarrow \mathcal{L} = \mathcal{J}$), the sensitivities can be computed according to

$$\frac{d\mathcal{J}}{d\alpha} = \frac{\partial\mathcal{J}}{\partial\alpha} + \mathcal{V}^T\frac{\partial\mathcal{G}}{\partial\alpha} \tag{2.4}$$

Basically, adjoint methods can be divided into two categories: The discrete and the continuous approach which mainly differ in the order of the discretization and linearization step of the governing PDEs. The different approaches are illustrated in Figure 2.1.

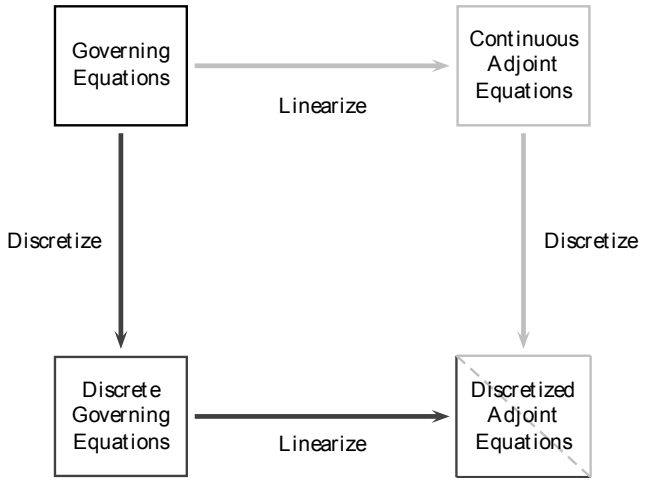

Figure 2.1: Discretization and linearization compared for the discrete and continuous adjoint approach [6]

2.1 The Discrete Approach

In the case of the discrete approach, the discrete adjoint system is derived based on the discretized governing equations. Using the implementation of the solution scheme, Algorithmic Differentiation (AD) can be applied to get the required derivatives. Therefore, the mathematical effort to obtain derivatives is relatively small and the results are exact up to machine accuracy. Since the process can be automated, it can be easily applied to arbitrary complex cost functionals. On the other hand, high computational costs, especially memory consumption [7], may occur and one has only a slight flexibility regarding the solution of the arising systems which can become highly stiff or ill-conditioned [6].

The solution scheme for the discretized state equations should lead to vanishing residuals everywhere in the computational domain. Since the boundary conditions already enter the scheme, they are automatically contained. Therefore we have $\mathcal{G} = \{\mathcal{R}_k\} = 0$. The Lagrangian then reads

$$\mathcal{L} = \mathcal{J}_D + \sum_{k=1}^{N} \psi_k^T \mathcal{R}_k. \tag{2.5}$$

One notes that we have $\mathcal{L} = \mathcal{J}_D$, if the constraints are fulfilled, i.e. $\mathcal{G} = \{\mathcal{R}_k\} = 0$. For the perturbation one gets

$$\Delta\mathcal{L} = \Delta\mathcal{J}_D + \sum_{k=1}^{N} \psi_k^T \Delta\mathcal{R}_k. \tag{2.6}$$

The linearization of $\Delta\mathcal{J}_D$ and $\Delta\mathcal{R}_k$ yields

$$\Delta\mathcal{J}_D = \sum_{l=1}^{N} \frac{\mathfrak{D}\mathcal{J}_D}{\mathfrak{D}U_l}\Delta U_l + \frac{\mathfrak{D}\mathcal{J}_D}{\mathfrak{D}\alpha}\Delta\alpha \tag{2.7}$$

$$\Delta\mathcal{R}_k = \sum_{l=1}^{N} \frac{\mathfrak{D}\mathcal{R}_k}{\mathfrak{D}U_l}\Delta U_l + \frac{\mathfrak{D}\mathcal{R}_k}{\mathfrak{D}\alpha}\Delta\alpha \tag{2.8}$$

Plugging in this terms into equation (2.6) gives

$$\Delta\mathcal{L} = \left(\frac{\mathfrak{D}\mathcal{J}_D}{\mathfrak{D}\alpha} + \sum_{k=1}^{N} \psi_k^T \frac{\mathfrak{D}\mathcal{R}_k}{\mathfrak{D}\alpha}\right)\Delta\alpha + \sum_{k=1}^{N}\left(\frac{\mathfrak{D}\mathcal{J}_D}{\mathfrak{D}U_k} + \sum_{l=1}^{N} \psi_l^T \frac{\mathfrak{D}\mathcal{R}_l}{\mathfrak{D}U_k}\right)\Delta U_k \tag{2.9}$$

As mentioned before, all terms which occur together with perturbations in the state variables should vanish. This leads to the adjoint equation

$$\sum_{l=1}^{N}\left(\frac{\mathfrak{D}\mathcal{R}_l}{\mathfrak{D}U_k}\right)^T \psi_l = -\left(\frac{\mathfrak{D}\mathcal{J}_D}{\mathfrak{D}U_k}\right)^T. \tag{2.10}$$

If this equation is fulfilled, we can conclude for our cost functional

$$\Delta\mathcal{J}_D = \Delta\mathcal{L} = \left(\frac{\mathfrak{D}\mathcal{J}_D}{\mathfrak{D}\alpha} + \sum_{k=1}^{N} \psi_k^T \frac{\mathfrak{D}\mathcal{R}_k}{\mathfrak{D}\alpha}\right)\Delta\alpha \tag{2.11}$$

and further

$$\frac{d\mathcal{J}_D}{d\alpha} = \frac{\mathfrak{D}\mathcal{J}_D}{\mathfrak{D}\alpha} + \sum_{k=1}^{N} \psi_k^T \frac{\mathfrak{D}\mathcal{R}_k}{\mathfrak{D}\alpha}. \tag{2.12}$$

The remaining terms are the explicit dependence of cost functional and state equations on the design variables. When the adjoint equation is solved, these dependences can be computed relatively cheaply to obtain the sensitivity of the cost functional with respect to the design variables.

2.2 The Continuous Approach

In case of the continuous approach, the analytical form of the state equations is used to derive the adjoint equations. The resulting system of equations is then discretized similarly as it is done for the state equations. The derivation on an analytical level requires a lot of mathematical effort and can become sophisticated for complex systems of state equations. However, one is free in the choice of a scheme for this system, since the obtained equations do not depend on the discretization of the state equations. On the other hand, the choice of cost functionals is limited and the gradient can be inaccurate.

For the derivation of the continuous adjoint equations, we assume that the system of PDEs $\mathcal{N}$ is fulfilled, i. e. $\mathcal{G} = \{\mathcal{N}\} = 0$. Furthermore, the continuous objective function $\mathcal{J}_C$ is defined either over the whole computational domain Ω or over the boundary Γ. One can write

$$\mathcal{J}_C = \int_\Omega j d\Omega \text{ or } \mathcal{J}_C = \int_\Gamma j d\Gamma. \tag{2.13}$$

For the Lagrangian one gets

$$\mathcal{L} = \mathcal{J}_C - \int_\Omega \phi^T \mathcal{N} d\Omega. \tag{2.14}$$

A perturbation in the design α leads to perturbations in the state variables as well as in the corresponding domain and boundary. For the perturbed Lagrangian it follows:

$$\delta\mathcal{J} = (\mathcal{J}_c' - \mathcal{J}_c) - \left(\int_{\Omega'} \phi^T \mathcal{N}' d\Omega - \int_\Omega \phi^T \mathcal{N} d\Omega \right) \tag{2.15}$$

Again, the next step is to transform this equation such that terms including perturbations in the state δU are isolated. Once this is done, one can set conditions such that these terms vanish. According to whether these conditions are defined over the domain or the boundary, they are referred to as adjoint equations or adjoint boundary conditions, respectively. Knowing or being able to easily calculate the remaining terms, one can now compute the sensitivity information of the objective function regarding changes in the design. Since the specific state equations and boundary conditions directly enter equation (2.15), the derivation of the adjoint equations cannot be generally done. One should note that each change in the state equations or boundary conditions requires a new derivation of adjoint equations.

To illustrate the proceeding, one part of the derivation for some flow equations is presented in the following. For a stationary incompressible problem, the continuity equations for the state variable $U = u$ (velocity) is given as

$$\mathcal{N} = -\frac{\partial u_j}{\partial x_j} = 0, \tag{2.16}$$

where the Einstein notation was used. For the Lagrangian, it follows

$$\mathcal{L} = \mathcal{J}_C + \int_\Omega \phi^T \mathcal{N} d\Omega. \tag{2.17}$$

The derivative of $\mathcal{L}$ with respect to the i-th design variable α_i is then given by

$$\frac{d\mathcal{L}}{d\alpha_i} = \frac{d\mathcal{J}_\mathcal{C}}{d\alpha_i} + \frac{d}{d\alpha_i} \left(\int_\Omega \phi \mathcal{N} d\Omega \right). \tag{2.18}$$

With the Leibniz integral rule, it follows:

$$\frac{d\mathcal{L}}{d\alpha_i} = \frac{d\mathcal{J}_\mathcal{C}}{d\alpha_i} + \int_\Omega \phi \frac{\partial \mathcal{N}}{\partial \alpha_i} d\Omega + \int_\Gamma \phi \mathcal{N} n_j \frac{dx_j}{d\alpha_i} d\Gamma. \tag{2.19}$$

The partial derivative of $\mathcal{N}$ with respect to the i-th design variable reads

$$\frac{\partial \mathcal{N}}{\partial \alpha_i} = -\frac{\partial}{\partial \alpha_i} \left(\frac{\partial u_j}{\partial x_j} \right) = -\frac{\partial}{\partial x_j} \left(\frac{\partial u_j}{\partial \alpha_i} \right) \tag{2.20}$$

Thus, we have

$$\int_\Omega \phi \frac{\partial \mathcal{N}}{\partial \alpha_i} d\Omega = -\int_\Omega \phi \frac{\partial}{\partial x_j}\left(\frac{\partial u_j}{\partial \alpha_i}\right) d\Omega, \tag{2.21}$$
$$= -\int_\Gamma \phi \frac{\partial u_j}{\partial \alpha_i} n_j d\Gamma + \int_\Omega \frac{\partial \phi}{\partial x_j}\frac{\partial u_j}{\partial \alpha_i} d\Omega.$$

Now, we have isolated the terms corresponding to a perturbation in the state variables $\frac{\partial u_j}{\partial \alpha_i}$ and we can set the multipliers to zero. For the field integral, we claim $\frac{\partial \phi}{\partial x_j} = 0$. Together with further conditions arising from the remaining state equations, the adjoint equations are obtained. Similarly, the terms of boundary integrals will lead to the boundary conditions for the adjoint variables.

2.3 The Hybrid Approach

As mentioned before, the continuous and discrete adjoint approach often show opposing characteristics. The observed advantages and disadvantages of all approaches are listed in Figure 2.2. The hybrid approach mainly aims at combining these two approaches such that

	Discrete	Continuous	Hybrid
Ease of development[21, 22, 25–27]	+	−	±
Compatibility of numerical gradients:			
- with the discretized PDE[9, 21, 26–28]	+	−	−
- with the continuous PDE[26, 29]	−	+	+
Surface formulation for gradients[28, 30]	−	+	+
Ability to handle:			
- arbitrary functionals[22, 27]	+	−	±
- non-di erentiability[22, 26, 27, 31]	+	−	+
Computational cost[13, 21, 26, 27]	−	+	±
Flexibility in solution[21, 22, 26, 29, 32]	−	+	±

Figure 2.2: Simple comparison of the different approaches [6]

the advantages of both approaches are maintained. Particularly, one tries to decrease the mathematical effort to derive an adjoint method and to lower the computational requirements. The idea is further that a hybrid method should conserve the flexibility and quality of the solution scheme of a continuous method and the ability to handle complex PDEs and non-differentiability of a discrete method. The general scheme of the hybrid approach is sketched in Figure 2.3.

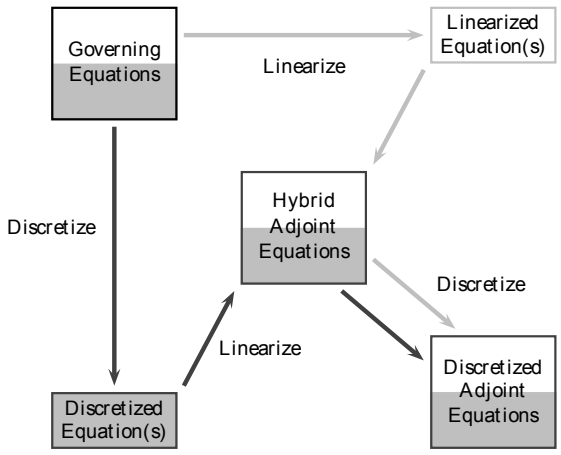

Figure 2.3: Schematic sketch of the hybrid adjoint approach [6]

For the hybrid approach the state equations are composed of one continuous and one discrete part, i.e.

$$\mathcal{G} = \{\{\mathcal{N}\}_C, \{\mathcal{R}_k\}_D\} = 0 \tag{2.22}$$

The idea is then that equations which are not affected by small changes in the state equations and which are easy to differentiate will enter the continuous part. The remaining equations which are not (easily) differentiable or are planed to be modified enter the discrete part. If one follows this approach and has once derived the continuous adjoint equations, variations of the original problem will not require a huge development effort, but one will be allowed to reuse the majority of the already existing functionality. For the hybrid objective function a combined version of continuous and discrete objective function is introduced:

$$\mathcal{J}_H = \beta \mathcal{J}_C + (1-\beta)\mathcal{J}_D \tag{2.23}$$

This function is meant to be either fully continuous ($\beta = 1$) or fully discrete ($\beta = 0$). Thus, the variable $\beta = \{0, 1\}$ serves as switch. The Lagrangian function containing both the continuous and discrete part of the state equations is given as:

$$\mathcal{L} = \beta \mathcal{J}_C + (1-\beta)\mathcal{J}_D - \int_\Omega \varphi_C^T \mathcal{N}_C d\Omega + \sum_{k=1}^{N} \varphi_{D,k}^T \mathcal{R}_{D,k} \tag{2.24}$$

The perturbation then yields

$$\begin{aligned} \{\delta, \Delta\}\,\mathcal{L} =& \beta(\mathcal{J}_C' - \mathcal{J}_C) + (1-\beta)\Delta\mathcal{J}_D && (2.25)\\ &- \left(\int_{\Omega'} \varphi_C^T \mathcal{N}_C' d\Omega - \int_\Omega \varphi_C^T \mathcal{N}_C d\Omega\right) \\ &+ \sum_{k=1}^{N} \varphi_{D,k}^T \Delta\mathcal{R}_{D,k}. && (2.26) \end{aligned}$$

The next step follows again the same idea as used before in the continuous and discrete approach. Based on equation (2.26) one identifies terms containing perturbations in the state variables δU and ΔU. Then, these terms have to vanish and thereby the adjoint equation and boundary conditions are obtained for the adjoint variables φ_C and φ_D.

Before one can start to derive a hybrid adjoint method for a specific problem, one has mainly two degrees of freedom. The first one is the choice of the equations that enter either the continuous or discrete part of the hybrid state equations. The second one is the decision between a continuous or a discrete objective function.

3 Application to Turbulent Flow Simulations

3.1 Problem Description

As a test case, the transonic flow over the RAE 2822 airfoil at non-zero angle-of-attack has been investigated in [6]. It was used to compare the continuous approach with the full hybrid approach. For the continuous approach, the frozen turbulence assumption, which will be explained later, is made. The computational mesh which was used for the test case consists of 13 937 points, where 192 points shape the surface, and is shown in Figure 3.1.

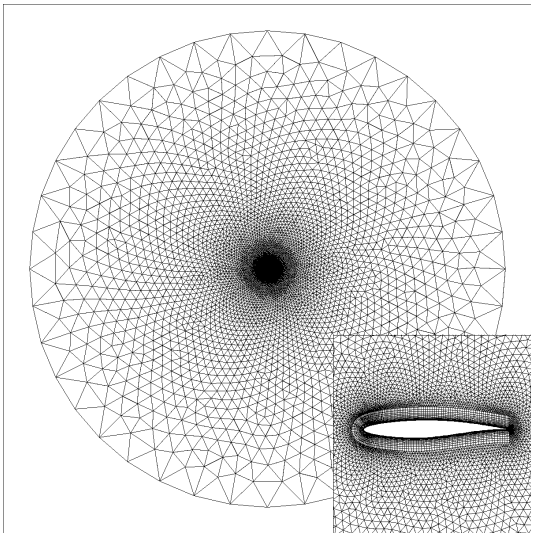

Figure 3.1: Computational mesh around the airfoil [6]

For the modeling of the flow, one can use the Reynolds-Averaged Navier-Stokes equations for compressible flow together with a turbulence model. The corresponding equations, composed of one part for the mean flow (subscript L) and one part for the turbulence model (subscript T), can be written as

$$\mathcal{N}(U, \partial_j U, \alpha) = \begin{pmatrix} \mathcal{N}_L \\ \mathcal{N}_T \end{pmatrix} = 0, \text{ in } \Omega \tag{3.1}$$

with state variables

$$U = \begin{pmatrix} U_L \\ U_T \end{pmatrix}, \tag{3.2}$$

gradients of the state variables $\partial_j U$ and design variables α.

The mean flow equations for the mean flow variables

$$U_L = \begin{pmatrix} \rho \\ \rho u_i \\ \rho E \end{pmatrix}, \tag{3.3}$$

are given as

$$\mathcal{N}_L(U, \partial_j U, \alpha) = \partial_i (F_i - \mu^{v1} F_i^{v1} - \mu^{v2} F_i^{v2}) = 0, \text{ in } \Omega \tag{3.4}$$

with flux terms

$$F_i = \begin{pmatrix} \rho u_i \\ \rho u_i u_j + p\delta_{ij} \\ \rho u_i H \end{pmatrix}, F_i^{v1} = \begin{pmatrix} 0 \\ \tau_{ij} \\ u_k \tau_{ik} \end{pmatrix}, F_i^{v2} = \begin{pmatrix} 0 \\ 0 \\ C_p \partial_i T \end{pmatrix}. \tag{3.5}$$

The stress tensor is defined by

$$\tau_{ij} = (\partial_j u_i + \partial_i u_j) - \frac{2}{3}\delta_{ij}\partial_k u_k \tag{3.6}$$

and the temperature for an ideal gas is given as

$$T = \frac{p}{R\rho}. \tag{3.7}$$

For the viscosity terms we have

$$\mu^{v1} = \mu + \mu_T, \ \mu^{v2} = \frac{\mu}{Pr} + \frac{\mu_T}{Pr_T}, \tag{3.8}$$

with the laminar and turbulent Prandtl number Pr or Pr_T. The representation of the so called eddy viscosity μ_T depends on the turbulence model. It is assumed that only μ_T couples the mean flow equations and the turbulence model.

Next, a general representation for a turbulence model is given as

$$\mathcal{N}_T(U, \partial_j U, \alpha) = \partial_i F_{T_i} - S_T = 0, \text{ in } \Omega, \tag{3.9}$$

with flux term F_{T_i} and source term S_T. Depending on the specific model, this representation contains one or multiple equations. The solution of these equations will then allow us to compute the eddy viscosity μ_T and can in general depend on $U, \partial_j U$ and α.

The application of the continuous adjoint approach to a turbulence model is very challenging. A widely used assumption is that the variation of the eddy viscosity can be neglected and, thus, the influence on the sensitivities arising from the turbulence effects is dropped. This assumption is also known as the frozen turbulence assumption. However, for the Spalart-Allmaras model a continuous adjoint formulation was derived by Zymaris et al. [9].

One of the main achievements of the hybrid approach is now that one has the possibility to treat the mean flow equations continuously and the equations of the turbulent model discretely. This not only saves the effort for the analytical derivation of the continuous adjoint equations but also lowers the costs for the adaption of the adjoint method in the case of switching the turbulence model. If one applies AD for the discrete part, the models can be seen more or less as black boxes. However, the mean flow equations still depend explicitly on the eddy viscosity μ_T and, thus, also on the specific turbulence model. This remaining model dependence in the mean flow equations is removed by introducing an additional equation for the eddy viscosity:

$$\mathcal{N}_{\mu T}(U, \partial_j U, \alpha) = \mu_T - f = 0, \text{ in } \Omega \tag{3.10}$$

with

$$f(U, \partial_j U, \alpha) = \mu_T \tag{3.11}$$

Thus, the explicit dependence on the form of μ_T is moved from the continuous to the discrete part.

Applying the steps described in the previous sections to this set of equations, one obtains a continuous-like PDE with additional discrete and mixed source terms for the adjoint variables corresponding to the mean flow. Additionally, one gets a set of hybrid boundary conditions. These equations are solved like a traditional PDE. Furthermore, a discrete-like linear system with mixed source terms can be derived for the turbulence related adjoint

variables and, again, this system is treated like a conventional linear system. It has to be noted that no model-dependent derivatives of the eddy viscosity appear in the continuous part and, thus, these terms only enter the discrete part. Since AD can be used to compute the required derivatives, the mathematical form of the hybrid adjoint is not depending on the specific turbulence model. Finally, the adjoint solution can be used to evaluate the sensitivity of the objective function with respect to changes in the surface shape of the airfoil.

3.2 Results

In this section, the results obtained for the described test case are summarized. The main flow conditions for this case are given in the following:

- Freestream Mach number $M_\infty = 0.754$
- Angle of attack, $\hat{\alpha} = 2.57°$
- Reynolds number $Re = 6.2 \cdot 10^6$

As turbulence model, the one-equation Spalart-Allmaras model was used. The simulation of the flow equations has been iterated until the residuals reached machine accuracy. The solution for the adjoint variable has been stopped after the changes in the geometric sensitivity varied by less than 10^{-6} over 100 iterations.

In Figure 3.2 the sensitivities of the drag coefficient with respect to perturbations in the surface are plotted for both approaches. For the lower surface, the values are very similar. However, significant differences can be seen on the upper surface in the region of the typical shock. The parametrization of the shape was done by using 38 Hicks-Henne bump functions.

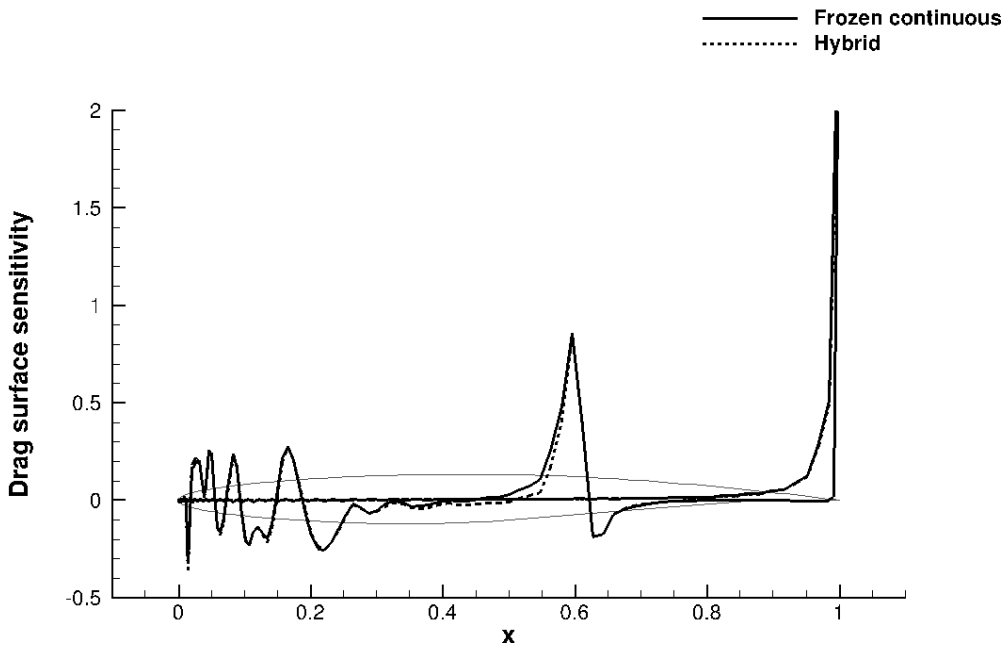

Figure 3.2: Surface sensitivity of drag coefficient [6]

The bumps are numbered clockwise starting from trailing edge on the lower side. The shape sensitivities obtained by each of the adjoint approaches are compared with finite differences results in Figure 3.3. The values clearly differ for the bumps 18 - 34. Additionally, the finite differences results have been validated using a varying step size.

Based on the sensitivities, a shape optimization has been performed. The objective was to minimize the drag of the airfoil. As a further constraint, the lift had to be kept constant. As gradient based optimization method, a simple quasi-Newton method was utilized. The results for the evolution of the drag and lift coefficient over 15 optimization steps are shown in Figure 3.4. Using the sensitivities obtained by the frozen continuous approach, the drag coefficient could be decreased about 47 % with a lift to drag ratio of 55.6. For the hybrid approach, the drag coefficient was decreased about 52 % with a lift to drag ratio of 61.8. The original lift to drag ratio was 28.6. The original and optimized shapes of the airfoil are compared in Figure 3.5. Again, the results mainly differ in the shock region on the upper surface.

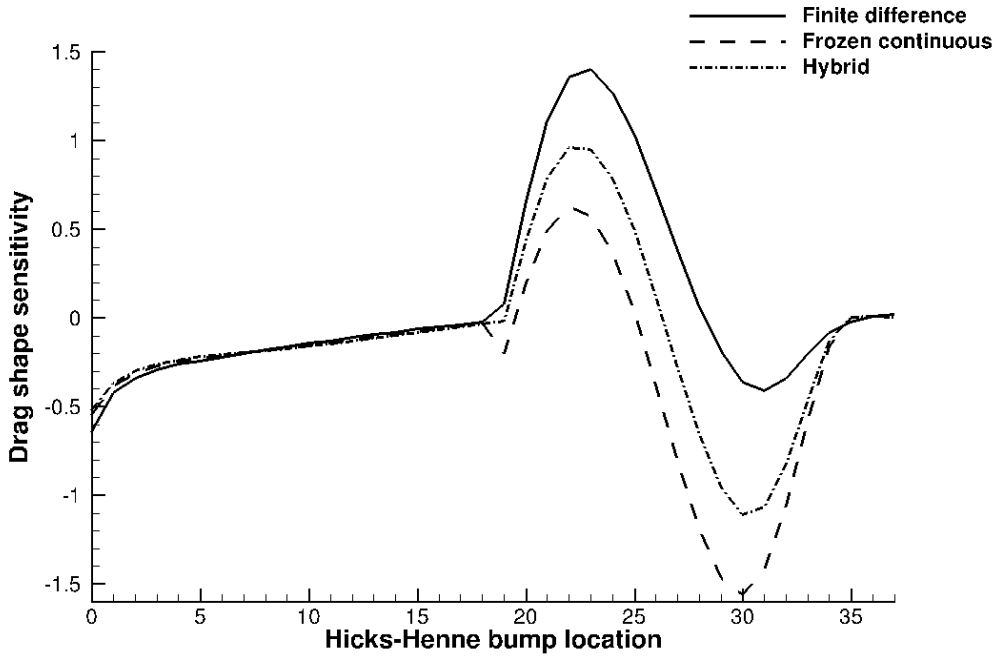

Figure 3.3: Shape sensitivity of drag coefficient [6]

It has also to be mentioned, that, if the turbulence effects have no significant influence, the frozen continuous and the hybrid approach give very similar results [6]. Furthermore, the improvement of the shape regarding drag and lift also does not differ that much as in the case presented here.

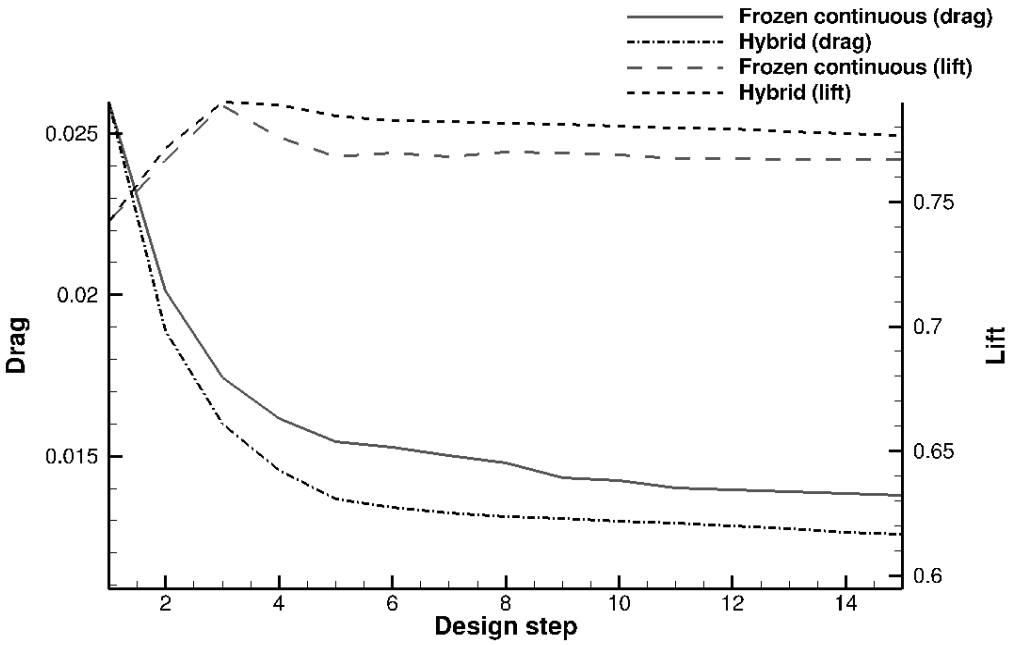

Figure 3.4: Drag and lift coefficient during the shape optimization process [6]

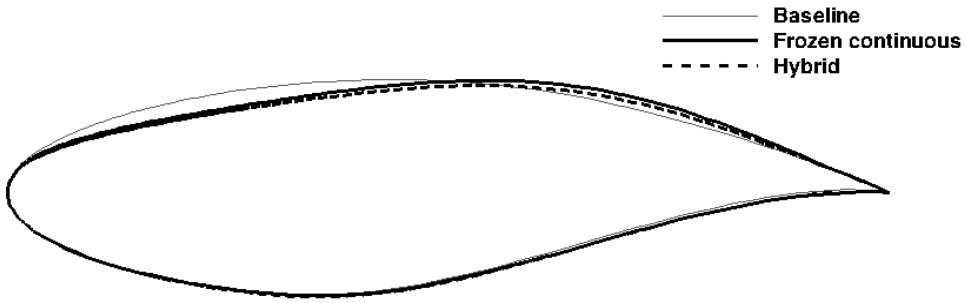

Figure 3.5: Comparison of original and optimized shapes after 10 design steps [6]

4 Conclusion

In this work, the basics of shape optimization have been described to motivate the use of adjoint methods. A brief description of the discrete and continuous adjoint approach was given. Based on the characteristics of both approaches, the idea and the motivation of a hybrid adjoint approach have been outlined. Finally, the application of this approach to a test case and the comparison of the obtained result with a classical adjoint approach have been presented. One can conclude, that the main idea of a hybrid approach is to combine the advantages of both the discrete and the continuous approach, e.g. lowering the mathematical effort for its derivation and the computational requirements. This can be achieved by assigning equations that are not expected to change to the continuous part and treating complex and varying parts of the problem discretely.

Bibliography

[1] R. E. Burkard and U. Zimmermann. Gradienten- und Newton-Verfahren. In *Einführung in die Mathematische Optimierung*, volume 5045 of *Springer-Lehrbuch*, pages 285–296. Springer Berlin Heidelberg, 2012.

[2] N. R. Gauger. Efficient Deterministic Approaches for Aerodynamic Shape Optimization. In D. Thévenin and G. Janiga, editors, *Optimization and Computational Fluid Dynamics*, pages 111–145. Springer Berlin Heidelberg, 2008.

[3] K. C. Giannakoglou and D. I. Papadimitriou. Adjoint Methods for Shape Optimization. In D. Thévenin and G. Janiga, editors, *Optimization and Computational Fluid Dynamics*, pages 79–108. Springer Berlin Heidelberg, 2008.

[4] C. Othmer. A continuous adjoint formulation for the computation of topological and surface sensitivities of ducted flows. *International Journal for Numerical Methods in Fluids*, 58(1770):861 – 877, 2008.

[5] T. W. Taylor, F. Palacios, K. Duraisamy, and J. J. Alonso. Towards a Hybrid Adjoint Approach for Arbitrarily Complex Partial Differential Equations. In *42nd AIAA Fluid Dynamics Conference and Exhibit, New Orleans, Louisiana, USA*, 2012.

[6] T. W. Taylor, F. Palacios, K. Duraisamy, and J. J. Alonso. A hybrid adjoint approach applied to turbulent flow simulations. In *21st AIAA Computational Fluid Dynamics Conference, San Diego, CA*, 2013.

[7] M. Towara and U. Naumann. A Discrete Adjoint Model for OpenFOAM. *Procedia Computer Science*, 18(0):429 – 438, 2013. 2013 International Conference on Computational Science.

[8] M. Ulbrich and S. Ulbrich. *Nichtlineare Optimierung*. Mathematik Kompakt. Springer Basel, 2012.

[9] A. Zymaris, D. Papadimitriou, K. Giannakoglou, and C. Othmer. Continuous adjoint approach to the spalartallmaras turbulence model for incompressible flows. *Computers & Fluids*, 38(8):1528 – 1538, 2009.